

Efficient Task Allocation Protocol for a Hybrid-Hierarchical Spatial-Aerial-Terrestrial Edge-Centric IoT Architecture

Abbas JAMALIPOUR^{†a)}, Fellow and Forough SHIRIN ABKENAR^{†b)}, Nonmember

SUMMARY In this paper, we propose a novel Hybrid-Hierarchical spatial-aerial-Terrestrial Edge-Centric (H²TEC) for the space-air integrated Internet of Things (IoT) networks. (H²TEC) comprises unmanned aerial vehicles (UAVs) that act as mobile fog nodes to provide the required services for terminal nodes (TNs) in cooperation with the satellites. TNs in (H²TEC) offload their generated tasks to the UAVs for further processing. Due to the limited energy budget of TNs, a novel task allocation protocol, named TOP, is proposed to minimize the energy consumption of TNs while guaranteeing the outage probability and network reliability for which the transmission rate of TNs is optimized. TOP also takes advantage of the energy harvesting by which the low earth orbit satellites transfer energy to the UAVs when the remaining energy of the UAVs is below a pre-defined threshold. To this end, the harvested power of the UAVs is optimized alongside the corresponding harvesting time so that the UAVs can improve the network throughput via processing more bits. Numerical results reveal that TOP outperforms the baseline method in critical situations that more power is required to process the task. It is also found that even in such situations, the energy harvesting mechanism provided in the TOP yields a more efficient network throughput.

key words: fog computing, Internet of Things (IoT), unmanned aerial vehicles (UAVs), low earth orbit (LEO) satellites, energy harvesting (EH), k-means clustering

1. Introduction

With the exponential growth of the Internet of Things (IoT) demands, the need for providing reliable services with the lowest delay is sensed more. The paramount step in improving the efficiency of the IoT networks, comprising energy-constrained nodes with delay-sensitive tasks, was the emergence of fog computing [1] as a new paradigm in these networks. Fog nodes (FNs) are resource-rich nodes that provide complementary resources to the IoT nodes, also known as terminal nodes (TNs), at the edge of the network. Thereby, the TNs consume less energy to send their tasks to the FNs, rather than the data centers (DCs) in the cloud center. Moreover, it takes less time for a task to be transmitted to an FN for further processing [1].

Apart from the importance of fog computing to the IoT networks, the type of FNs significantly affects the performance of Fog-IoT networks. Much of the research efforts have been devoted to investigating the role of fixed FNs in

IoT networks. For example, Yousefpour et al. [2] design an optimal offloading policy to minimize delay in Fog-IoT networks. The authors in [3], [4] improve the network delay while considering the load balancing among FNs in the network. The main focus of the proposed method in [5], on the other hand, is to find a trade-off between energy consumption and delay in Fog-IoT networks. The proposed methods in [6], [7] take advantage of the caching mechanism to alleviate the network delay considering the energy constraints in the network. Network function virtualization (NFV) is another efficient method to optimize resource allocation in communication networks. To this end, Raveendran et al. propose an NFV-based mechanism in [8] which accordingly provides quality of service (QoS) requirements in the network. The efficiency of the Fog-IoT networks is not only limited to energy consumption and delay. Two different methods, one based on the optimization problem and the other based on reinforcement learning (RL) mechanism, are proposed in [9] to improve the throughput of Fog-IoT networks. Ramezani et al. propose mechanisms to improve the network throughput in energy harvesting (EH) [10], and backscattering [11].

The research body conducted in recent years show that the flexible nature of mobile FNs, including vehicles equipped with on-board units (OBUs) [12] and/or aerial vehicles, such as drones or unmanned aerial vehicles (UAVs) [13], enables them to reduce their distance with the TNs and hence, improve the energy efficiency of TNs, as well as the network delay. We thoroughly investigate the role of aerial FNs in Sect. 2.1.

The other issue that threatens the IoT networks is providing the QoS requirements in sparsely populated areas, such as valleys and mountains, where installing the fixed FNs is hard or impossible. To cope with this challenge, the spatial FNs have been introduced to the IoT networks as the other type of mobile FNs where the different types of satellites, such as geostationary orbit or geosynchronous equatorial orbit (GEO), medium earth orbit (MEO), and low earth orbit (LEO) satellites are leveraged as FNs to provide QoS in the Fog-IoT networks. This is while the low energy consumption, as well as the propagation delay, of the LEO satellites give them a higher priority than the GEO and the MEO satellites to play the role of FNs in the network [14]. However, the distance between the satellites and the TNs is still large enough to degrade the performance of Fog-IoT networks. To tackle this shortage, a large number of research have been conducted in order to investigate the impact of spatial-aerial integrated FNs on providing QoS for Fog-IoT

Manuscript received June 29, 2021.

Manuscript revised July 14, 2021.

Manuscript publicized August 17, 2021.

[†]The authors are with the WiNG Lab, the School of Electrical and Information Engineering, The University of Sydney, Sydney, NSW, 2006 Australia.

a) E-mail: a.jamalipour@ieee.org

b) E-mail: forough.shirinabkenar@sydney.edu.au

DOI: 10.1587/transcom.2021CEI0001

networks [15]. We thoroughly review the corresponding investigations in Sect. 2.2.

1.1 Motivation

Although many researchers have studied and addressed the major problems of providing QoS in the Fog-IoT network by leveraging spatial and aerial FNs, these FNs, especially the aerial FNs, suffer from a limited energy budget that needs to be addressed optimally. Moreover, the reliability of the network is another requirement that should be considered alongside other paramount parameters, such as delay and energy consumption. However, a few research have been carried out to analyze the reliability of Fog-IoT networks with respect to mobile FNs.

1.2 Contribution

The shortage of the proposed methods in the literature motivated us to propose an efficient architecture and protocol to provide remarkable QoS requirements, such as delay, energy efficiency, and reliability to the Fog-IoT networks. The contributions of this paper include:

- First of all, we propose a novel architecture, named Hybrid-Hierarchical spatial-aerial-Terrestrial Edge-Centric (H^2TEC), for the IoT networks. Figure 1 indicates H^2TEC architecture which comprises six groups of components, namely TNs, terrestrial base stations (BSs), UAVs, LEO satellites, GEO satellites, and cloud. We accordingly introduce the layered structure of H^2TEC in which the communications between different components are defined.
- The novel Task allOcation Protocol (TOP) is proposed by which the TNs form clusters based on the k-means clustering method. A UAV is associated with each cluster and the TNs send their generated tasks to the corresponding UAV. According to the assumptions of TOP, each UAV can only be assigned to one cluster at

a time slot. Moreover, each cluster is served by one and only one UAV in each time slot. TOP provides an offloading policy by which the delay constraints are met for the tasks generated by TNs.

- An optimization problem is formulated in order to adjust the 3D placement of each UAV with respect to the corresponding cluster, as well as TNs, such that the energy consumption of TNs is minimized and the QoS requirements in terms of reliability, outage probability, and delay are provided in the network.
- After completion of the 3D adjustment of the UAVs, their energy consumption needs to be managed in a way that the network throughput is maximized. Due to the limited energy budget of the UAVs and the huge amount of energy that these nodes consume to fly towards the corresponding cluster, an alternative solution is required to compensate for this shortage. One of the best options to provide the required supplementary energy to the mobile aerial FNs is the energy harvesting (EH) mechanism. The LEO satellites can take advantage of solar power; thanks to their structure and condition. To the authors' best knowledge, no previous research has been carried out in this regard and this is the first work studying the EH between the LEO satellites and the UAVs in Fog-IoT networks. According to the assumptions of TOP, the LEO satellites can transfer the energy to the UAVs. Subsequently, the UAVs can use the harvested energy to process more bits and so increase the network throughput. To this end, a second optimization problem is formulated aiming at maximizing the network throughput by optimizing the harvested power and time by the UAVs.

1.3 Organization

The rest of this paper is organized as follows: Section 2 provides the literature review of the edge-centric IoT networks. The novel H^2TEC architecture is proposed in Sect. 3. Section 4 presents the system model. Section 5 includes the proposed TOP protocol. Numerical results are provided in Sect. 6. Finally, Sect. 7 concludes the paper.

2. Literature Review

2.1 UAV-Assisted Edge-Centric IoT Networks

The emergence of UAVs as mobile edge nodes in edge-enabled IoT networks could significantly improve the performance of these networks. UAVs, thanks to their mobile and flexible nature, can adjust their distance to the TNs [16] by which the network delay is reduced and the energy efficiency and throughput of TNs are optimized. Different research efforts have been carried out to investigate the role of UAVs in improving the efficiency of IoT networks.

A group of research aims to improve the performance of networks including a single UAV and multiple TNs. For

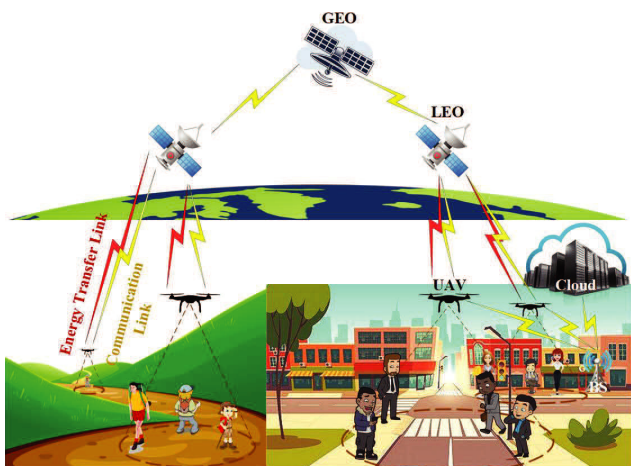


Fig. 1 H^2TEC architecture.

example, the proposed scheme in [17] assumes a fixed flight altitude for the UAV and aims to optimize the energy consumption of both the UAV and the TNs. To this end, a weight factor is defined by which the energy consumption of the TNs is prioritized. Wu et al. [18] propose an offloading strategy for a system model, including a single UAV and multiple TNs, by which the TNs optimally offload the tasks to the UAV. The main objective of the proposed strategy is to jointly optimize the UAV's 3D placement and the offloading size of tasks such that the energy efficiency of the UAV is improved. The authors in [19] consider a Fog-IoT network comprising one UAV and multiple TNs in which the UAV is equipped with an edge server to play the role of an FN. According to the assumptions of the proposed mechanism, each TN, depending on its own energy budget, is capable of either process its task locally or offload the task to the UAV for further processing. The main objective of the proposed task offloading mechanism is to optimally assign the tasks to the UAV such that the energy consumption for the UAV, as well as the TNs, is minimized while the delay constraints are met in the network. To this end, the trajectory of the UAV, which has a direct effect on the energy consumption of the UAV and the TNs, needs to be optimized. Hence, the optimal location of the UAV is found so that it covers a certain number of TNs, and also the corresponding TNs consume less energy for offloading the tasks to the UAV. Thereafter, the UAV stays hovering at a constant altitude for a time period to process the incoming tasks. Wang et al. [20] propose a mechanism which aims at maximizing the sum-rate, i.e., the total number of bits processed at the UAV, by jointly optimizing the allocation of the tasks generated by TNs to the UAV, the transmission power of TNs for offloading the tasks to the UAV, and the flight altitude of the UAV. The main objective of the proposed mechanism in [21] is to optimize the size of offloading data to the UAV, as well as the transmission rate of the TNs for transmitting the offloading portion of the tasks so that the energy consumption of both the UAV and the TNs are minimized.

The other group of investigations considers the system models comprising multiple UAVs and multiple TNs. For instance, Xu et al. [22] propose a mechanism wherein the UAVs are responsible to transfer the energy to the TNs for processing the tasks. However, the limited energy budget of the UAVs imposes limitations that need to be addressed by jointly optimizing the association of the UAV-TN with the time of transferring the energy. The authors in [23] propose a joint offloading method aiming at minimizing the total weighted consumed power of the system. The proposed method in [24] optimizes the transmission of all TNs are optimized so that they can receive the data from the corresponding UAV with the minimum loss. Mozzafari et al. [25] propose a framework in which the UAVs collaborate with the terrestrial BSs to improve the network delay. In another work carried out by the same authors [26], a new framework is proposed for a system in which the TNs are randomly activated to generate the tasks over time. The framework follows multi-fold objectives as optimizing the association between

the TNs and the UAVs, the 3D placement of the UAVs, the mobility of the UAVs, and the uplink power control such that the TNs consume less power consumption to transmit the generated tasks while the network path loss is minimized.

2.2 Hybrid Satellite-UAV-Assisted Edge-Centric IoT Networks

Satellite-air-ground integrated networks (SAGINs) were introduced to provide the required services for the TNs in places, such as valleys, where access to the terrestrial BSs is difficult or impossible. The LEO satellites play the role of BSs for the UAVs in such areas for which manage the UAVs. They also provide complementary resources for the UAVs to facilitate the processing of the tasks generated by the TNs [15].

Different research efforts have been devoted to investigating the effects of inter-operation of UAVs and satellites on improving the performance of edge-enabled IoT networks. For example, Hua et al. [27] consider a system in which the TNs can process the tasks locally or offload them to the higher layers. UAVs and satellites are leveraged to offload the tasks to the edge servers and the cloud servers, respectively. The criteria behind optimal task offloading are to jointly optimize the resource allocation in the network. However, many problems threaten such an optimization that we can remark the incomplete information and coupling between long-term constraints of queuing delay and short-term decision making. To deal with these challenges, the authors propose a learning-based queue-aware task offloading and resource allocation algorithm (QUARTER) by which network throughput is maximized while delay constraints are met.

The authors in [28] propose a learning-based approach for a highly dynamic environment to optimally offload the computation-intensive application to the upper layers. To this end, the corresponding UAVs and the satellites are used to offload the tasks to the edge servers and the cloud servers, respectively. Moreover, a joint task scheduling and resource allocation approach is proposed to optimally and efficiently allocate the resources to the virtual machines (VMs) for further processes.

The main objective of the proposed scheduling mechanism in [29] is to minimize the maximum computation delay among TNs. In this regard, the UAVs are leveraged to provide low-delay edge computing services to TNs. On the other hand, satellites facilitate access to the cloud servers for the TNs. To achieve the main goal defined by the mechanism, the association between the nodes in the network is controlled; the transmission power, bandwidth allocation, and resource allocation are optimized; and the position of the UAVs is efficiently adjusted.

Caching is a promising method in satellite-UAV-assisted networks. For instance, Gu et al. [30] consider a system, where the UAV is responsible for collecting data from the TNs, and the LEO satellite is used to broadcast data. Due to the low-power property of the TNs, the loss proba-

bility increases in the network. To cope with this problem, caching and repairing the data is an efficient solution. Moreover, it is necessary to protect the system's availability. To this end, an intelligent optimization is proposed which employs the fault-tolerant codes to address the problems of the lower availability by minimizing the communication costs in terms of power costs of the UAV and TNs.

3. Proposed Hybrid-Hierarchical Spatial-Aerial-Terrestrial Edge-Centric IoT Architecture

In this section, we propose a Hierarchical architecture for edge-centric IoT networks, named H²TEC architecture. Figure 1 shows the architecture of H²TEC including two different scenarios as follows:

- The left sub-figure in Fig. 1 shows a scenario including an environment in which installing the terrestrial BSs is not cost-efficient and also the BSs cannot be reached everywhere easily by the UAVs. The large coverage area of the LEO satellites makes them enable to play the role of the destination servers for the TNs. However, the large distance between the TNs and the LEO satellites imposes a huge delay on the tasks generated by the TNs. Moreover, the TNs need to consume a significant amount of energy to offload their tasks to the LEO satellites. To tackle these issues, UAVs are leveraged to serve TNs efficiently. The flexible nature of UAVs in approaching the TNs improves the network performance significantly [31], [32].
- In contrast, the right sub-figure in Fig. 1 indicates a city as an environment where terrestrial BSs are installed. In such a scenario, the UAVs are also leveraged as mobile FNs thanks to their flexibility and portability by which the processing delay of the tasks generated by the TNs is reduced. Also, the TNs need to consume less energy to transmit the tasks to the corresponding FN [33].

H²TEC comprises six main groups of components that are TNs, UAVs, Terrestrial BSs, LEO satellites, GEO satellites, and cloud. Figure 2 shows the layered architecture of H²TEC which includes four tiers, namely IoT layer, fog layer, fog management layer, and cloud layer. The IoT layer forms the lowest layer while the cloud layer is the topmost layer. In the following, the role of each layer in H²TEC is explained comprehensively.

3.1 IoT Layer

The TNs form the bottom layer with the lowest hierarchy of H²TEC, where a number of TNs group together to form a cluster. TNs are intuitively energy-constrained nodes that generate delay-sensitive tasks. Therefore, proper association of FNs with such energy-limited nodes can improve the energy consumption of TNs and also alleviate the processing delay of tasks generated by them. To tackle the aforementioned challenges, UAVs are leveraged as the mobile FNs in H²TEC to be assigned to each cluster and serve the tasks.

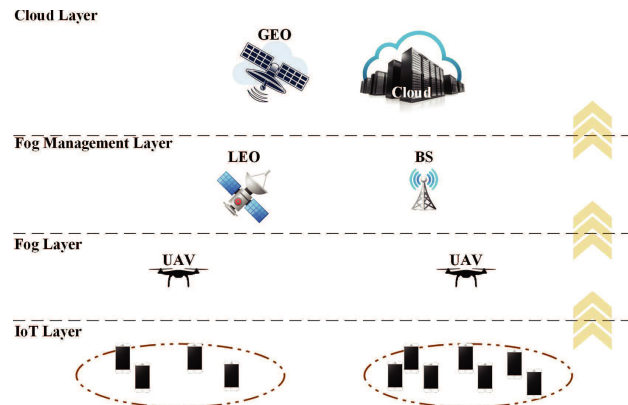


Fig. 2 Layered architecture of H²TEC.

3.2 Fog Layer

Fog layer is composed of UAVs that are referred to as the aerial type of mobile FNs in this paper. Rotary-wing UAVs are used in H²TEC, where each UAV is equipped with a single antenna. UAVs alleviate the energy consumption of TNs and reduce the processing delay of the tasks generated by them through flying towards the TNs and shortening their distance from the TNs. However, the computational capacity of the UAVs is limited for which they ask complementary resources from the manager FNs, i.e., the FNs located at the fog management layer. Moreover, the UAVs consume a huge amount of energy to fly [34]. To deal with the limited energy budget of the UAVs, the LEO satellite provided in the fog management layer transfer the energy to the UAVs for which the UAVs play the role of harvesters and harvest the power whenever their energy level is below a predefined threshold.

3.3 Fog Management Layer

Fog management layer includes manager FNs which are responsible to manage the FNs in the fog layer. There are two types of manager FNs in the management fog layer: (i) BSs as the terrestrial FNs; and (ii) LEO satellites as the spatial FNs.

Different types of BSs, such as radio towers and road side units (RSUs), are installed in the urban areas to cover the users. Each BS covers a specific region based on its own coverage range. Users, especially mobile users, who belong to a region communicate with the corresponding BS and forward their tasks to it for further process. The BS is resource-rich enough to serve the users. However, the large distance between the user and the corresponding BS degrades the QoS. To cope with such challenges, UAVs are leveraged as the mobile FNs closer to the TNs [33]. However, the limited computational resources of the UAVs impose limitations on them to provide sufficient resources for processing the tasks generated by the TNs. One solution is to communicate to the neighbor UAVs and use their resources as complementary resources. However, a direct connection between UAVs

is challenging due to the high mobility of these nodes. To this end, BSs are used as the manager FNs in H²TEC, not only to provide the complementary resources to the UAVs but also to manage them in the network and provide the communication requirements between different UAVs in the network.

Although BSs can manage the UAVs directly and easily, installing BSs in some places, such as valleys or rural areas, is difficult or impossible. To tackle such problems, LEO satellites are considered good replacements for the BSs. LEO orbit is closer to the earth than other orbits, especially GEO orbits. This causes the LEO satellites to consume less power than other types of satellites [35], [36]. Moreover, the LEO satellites can take advantage of the solar power satellite system to transfer the power to the ground BSs [37]. Therefore, the LEO satellites are leveraged to transfer the power to the UAVs when the energy budget of UAVs is lower than a threshold. Apart from the ability to provide energy harvesting in the system, the main advantage of LEO satellites refers to the low communication delay that these satellites provide. This feature arose of using the high-gain uniform planar array (UPA) antenna [36], [38]. Therefore, the UAVs can offload the tasks to the LEO satellites for further processing depends on the resource availability of the UAVs and delay constraints imposed on the tasks. However, the LEO satellites move very fast for which they are not visible for more than 20 or 30 minutes. This makes tracking of the LEO satellites challenging [36].

3.4 Cloud Layer

Cloud layer forms the topmost layer in H²TEC. GEO satellites and the cloud center are the fundamental components of the cloud layer.

GEO orbit is far from the earth compared to the LEO orbit. Hence, GEO satellites consume more energy than LEO satellites. Also, their communication delay is larger than the LEO satellites. GEO satellites manage the LEO satellites. However, GEO satellites are equipped with adequate computational resources thanks to their big size. Moreover, the large distance between them and the earth causes the GEO satellites to cover bigger regions than the LEO satellites, even including the LEO satellites [35], [36]. Considering the aforementioned advantages, GEO satellites are eligible to be defined as the centers for managing the LEO satellited in H²TEC. Hence, we call it in the H²TEC the mini satellite cloud. Although the computational capacity of the GEO satellites is much less than the cloud center, the policies, assumptions, and protocols provided in H²TEC yield a limited number of tasks are offloaded from the LEO satellites to the GEO satellites. Subsequently, the GEO satellites can manage the LEO satellites as the mini satellite cloud for which they can remove a LEO satellite if any failure happens to it, add a new LEO satellite, or transfer the energy to the LEO if it is required.

The cloud center on the other hand includes high-performance resource-rich DCs. However, the distance be-

tween the cloud DCs and the TNs is large. Therefore, the FNs are leveraged to provide the resources at the edge of the network. The cloud center has been provided in H²TEC to support the terrestrial BSs in the network. Therefore, if any BSs require complementary resources for processing the incoming tasks, it sends the tasks to the cloud for further processes [1].

4. System Model

We consider a Fog-IoT network including multiple terrestrial BSs, K LEO satellites, N UAVs, and M mobile TNs. The set of LEO satellites and UAVs are shown as $\mathcal{S} = \{s_1, s_2, \dots, s_K\}$ and $\mathcal{V} = \{v_1, v_2, \dots, v_N\}$, respectively.

TNs group together to form the clusters based on their location for which the k-means clustering [39] is used. In the considered system model, the coverage area of a UAV is a circle with a radius of \mathcal{R} that determines the size of a cluster. There is a direct direction between the flight altitude of a UAV and its coverage range so that by increasing the flight altitude, the coverage range of the UAV increases as well and vice versa. This is while by increasing the flight altitude, the outage probability of delivering the tasks generated by TNs to the corresponding UAV increases, the network reliability decreases, and the TNs need to consume more energy to offload their tasks to the UAV and suffer from larger delay. Hence, there exists a tradeoff between the flight altitude and the aforementioned parameters. It implies that finding the optimal flight altitude of the UAVs is an essential objective behind this work.

Each cluster c is composed of \mathbb{M}_c TNs, where $\text{TN}_{(i,c)}$ represents i -th TN belong to cluster c . Each $\text{TN}_{(i,c)}$ generates the tasks according to a Poisson point process (PPP) with the rate of $\nu_{(i,c)}(t)$ and the average size of $L_{(i,c)}$. The rate is a function of time that varies at each time slot t . For brevity, we omit t in the rest of this paper, e.g., $\nu_{(i,c)}$ stands for $\nu_{(i,c)}(t)$, unless the time-slot is emphasized. Among all available UAVs in the network, only one UAV is assigned to a cluster at a time slot. Besides, a UAV can only be assigned to one cluster at each time slot.

Notations: In this paper, scalars are denoted by italic letters. Boldface lower-case letters denote vectors. For a vector \mathbf{a} , $\|\mathbf{a}\|$, \mathbf{a}^T , and \mathbf{a}^H represent its Euclidean norm, its transpose, and its conjugate transpose, respectively. $\text{Tr}(\cdot)$ stands for the trace of a matrix. \mathbb{C} shows that a variable/vector is complex-valued. $\text{Pr}(\cdot)$ denotes the probability. $\Gamma(\cdot)$ and $\Gamma(\cdot, \cdot)$ denote the Gamma function and the upper incomplete Gamma function, respectively. Finally, $U[\cdot]$ indicates the uniform distribution.

4.1 Channel Model

In this section, we model the communication channels between TNs and UAVs, and UAVs and LEO satellites, separately by which we can obtain the outage probability, reliability, and energy harvesting model in the network.

4.1.1 Channel Model of a TN-UAV Pair

According to assumptions of the considered system model, the line-of-sight (LoS) propagation is established between a TN-UAV pair. Among all available practical distributions for the LoS transmission, the Nakagami- m distribution with the shape parameter m is a well-known model which can capture a wide range of fading scenarios ($m < 1$ for Hoyt, $m = 1$ for Rayleigh, and $m > 1$ for Rician) [40]–[42]. Therefore, the channel capacity between a TN and the corresponding UAV is defined as

$$C_{(i,c)j} = B \log_2 \left(1 + \frac{P_{(i,c)} g_0 \bar{h}_{(i,c)j} d_{(i,c)j}^{-\alpha}}{I_{(i,c)} + \sigma^2} \right), \quad (1)$$

where B is the bandwidth, $P_{(i,c)}$ is the transmission power of $\text{TN}_{(i,c)}$, g_0 denotes the channel gain at the reference distance $d_m = 1\text{m}$, α shows the path loss exponent, σ^2 is the additive white Gaussian noise (AWGN) power, and $\bar{h}_{(i,c)j}$ represents the fading coefficient of the channel, following Gamma distribution, with $\bar{h}_{(i,c)j} = 1$. $I_{(i,c)} = \sum_{\substack{i'=1 \\ i' \neq i}}^{M_c} P_{(i',c)} g_0 \bar{h}_{(i',c)j} d_{(i',c)j}^{-\alpha}$ is the interference derived from interfering TNs. Finally, $d_{(i,c)j}$ stands for the distance between $\text{TN}_{(i,c)}$ and v_j , which is given as

$$d_{(i,c)j} = \sqrt{z_j^2 + \|\mathbf{u}_j - \mathbf{u}_{(i,c)}\|^2}, \quad (2)$$

where z_j is the flight altitude of v_j , $\mathbf{u}_j = [x_j, y_j]^T$ and $\mathbf{u}_{(i,c)} = [x_{(i,c)}, y_{(i,c)}]^T$ are the horizontal coordinate/projection of v_j and $\text{TN}_{(i,c)}$, respectively. Moreover, the height of TNs is set to zero.

Since interference is dominant, we ignore the noise in our calculations. Therefore, signal to interference ratio (SIR) is expressed as

$$C_{(i,c)j} = B \log_2 \left(1 + \frac{P_{(i,c)} g_0 \bar{h}_{(i,c)j} d_{(i,c)j}^{-\alpha}}{I_{(i,c)}} \right), \quad (3)$$

4.1.2 Channel Model between UAVs and LEO Satellites

The channel model between a UAV and the corresponding LEO satellite follows the shadowed Rician (SR) [27], [42]. Similar to the TNs-UAVs pair, the LoS propagation is established between each UAV-LEO pair. Therefore, the channel capacity between UAV and the corresponding LEO satellite is modeled as

$$C_{jk} = B \log_2 \left(1 + \frac{P_j g_{kj}^2}{d_{jk}^2 \sigma^2} \right), \quad (4)$$

where P_j is the transmission power of v_j . Each LEO satellite is equipped with $N_x \times N_y$ UPA antennas, where N_x and N_y shows the number of antennas in x-axis and y-axis, respectively. Accordingly, $\mathbf{g}_{kj} \in \mathbb{C}^{N_x \times N_y}$ represents the fading coefficient of the channel, following Rician distribution. Finally, d_{jk} stands for the distance between v_j and s_k . Since

the altitude of the LEO satellite dominates both the flight altitude of UAV and the horizontal projection of the UAV, d_{jk} is given in terms of the altitude of s_k , i.e., $d_{jk} = z_k$.

4.2 Outage Probability Model

In the considered system model, if the transmission rate of a TN exceeds the channel capacity between the TNs and the corresponding UAV, the UAV is not able to receive the tasks. Therefore, the outage probability happens in the network. Accordingly, considering $R_{(i,c)}$ as the transmission rate of $\text{TN}_{(i,c)}$, the outage probability is defined as

$$P_{out} = \Pr (C_{(i,c)j} < R_{(i,c)}) \quad (5)$$

$$= \Pr \left(B \log_2 \left(1 + \frac{P_{(i,c)} g_0 \bar{h}_{(i,c)j} d_{(i,c)j}^{-\alpha}}{I_{(i,c)}} \right) < R_{(i,c)} \right).$$

We assume that the fading coefficient of all channels in a cluster is the same, i.e., $\bar{h}_{(i,c)j} = \bar{h}, \forall \text{TN}_{(i,c)} \in \text{cluster } c$. By employing the methods and assumptions provided in [43], we have

$$P_{out} = \frac{m^{(m-1)} A_1^{2m} \Gamma(2m, m\bar{h}^2)}{\Gamma^2(m)} - \frac{\Gamma(m, m\bar{h}^2)}{\Gamma(m)}, \quad (6)$$

where $A = (2^{R_{(i,c)j}/B} - 1) d_{(i,c)j}^\alpha \sum_{\substack{i'=1 \\ i' \neq i}}^{M_c} d_{(i',c)j}^{-\alpha}$.

4.3 Delay Model

Every task generated in the considered system model suffers from two types of delay. The first delay is the transmission delay for sending the generated task from the corresponding TN to the corresponding UAV; and the second type of delay, referred to as computing delay, is the required time for processing the task at the corresponding UAV. In the proposed architecture, the transmission rate reciprocity is held for all UAVs. Therefore, the transmission delay from the UAVs to the other nodes in the network is ignored. Moreover, we assume that the processing delay of tasks at the satellites and/or at the cloud is very small (relative to other system delays) so as is negligible.

By considering $L_{(i,c)}$ as the size of a task generated by $\text{TN}_{(i,c)}$, the transmission delay is given as

$$D_{(i,c)}^{tx} = \frac{L_{(i,c)}}{R_{(i,c)}}. \quad (7)$$

Assume that λ_j and L_j are the average traffic rate and the average size of tasks per arrival at v_j , respectively. By defining μ_j as the service rate of v_j , the required service time for $L_{(i,c)}$ at v_j is calculated as [44]

$$D_{(i,c)j}^{comp} = \frac{L_{(i,c)}}{\mu_j - \lambda_j L_j}. \quad (8)$$

Therefore, the total processing delay of a task is given as

$$D_{(i,c)} = \frac{L_{(i,c)}}{R_{(i,c)}} + \frac{L_{(i,c)}}{\mu_j - \lambda_j L_j}. \quad (9)$$

4.4 Reliability Model

The network is reliable if and only if the UAVs are available to the TNs. According to the definitions provided in [45], [46], the reliability is defined with respect to each TN as the probability that each UAV is operational to process the assigned task to it, and the probability that the communication link between each TN and UAV is operational during the communication period. We define ϑ_j as the failure rate of v_j which follows a Poisson process. Therefore, the reliability of sustainable communication between $\text{TN}_{(i,c)}$ and v_j is modeled as

$$\Upsilon_{(i,c)j}^{\text{comp}} = e^{-\vartheta_j \frac{L_{(i,c)}}{\mu_j - \lambda_j L_j}}. \quad (10)$$

On the other hand, $\omega_{(i,c)j}$ denotes the failure rate of the communication link between $\text{TN}_{(i,c)}$ and v_j which also follows the Poisson process. Hence, the reliability of processing a task generated by $\text{TN}_{(i,c)}$ at v_j is given as

$$\Upsilon_{(i,c)j}^{\text{comm}} = e^{-\omega_{(i,c)j} \frac{L_{(i,c)}}{R_{(i,c)}}}. \quad (11)$$

Finally, the reliability of processing $L_{(i,c)}$ at v_j is equal to the multiplication of $\Upsilon_{(i,c)j}^{\text{comm}}$ and $\Upsilon_{(i,c)j}^{\text{comp}}$:

$$\Upsilon_{(i,c)j} = e^{-\omega_{(i,c)j} \frac{L_{(i,c)}}{R_{(i,c)}} - \vartheta_j \frac{L_{(i,c)}}{\mu_j - \lambda_j L_j}}. \quad (12)$$

4.5 Energy Model

TNs and UAVs follow different energy models based on their role in the network. In this section, the energy models of TNs and UAVs are presented separately. It is worth mentioning that according to the assumption of the considered system model, BSs, satellites, and cloud have enough energy budget so as the energy constraints are not imposed on them.

4.5.1 Energy Model of TNs

The energy consumption of TNs refers to the required energy for transmitting a task to the corresponding UAV. Hence, the energy consumption of $\text{TN}_{(i,c)}$ is expressed as

$$E_{(i,c)} = P_i \frac{L_{(i,c)}}{R_{(i,c)}}. \quad (13)$$

4.5.2 Energy Model of UAVs

The energy consumption of a UAV is composed of two parts. The major part is the energy that the UAV consumes to fly towards the corresponding cluster, namely propulsion energy. The minor part is the communication-related energy, i.e., the energy consumption for processing the tasks. Since

the flight energy consumption is dominant on the processing energy consumption, the latter is usually ignored in the calculations [47]. However, as a novel contribution to our proposed architecture, the UAVs play the role of harvesters in the network for which they receive the power transferred by the LEO satellites. Since the EH procedure depends on the communication-related energy of the UAVs, we consider it in our calculations. Moreover, the harvesting energy of UAVs is represented in this section.

(1) Flight Energy Model

We assume that each UAV moves with a constant speed V towards the corresponding cluster. The center of a cluster shows the horizontal coordinate of the cluster, which is defined as the mean of coordinate of the TNs belong to the cluster, i.e., $\mathbf{u}_c = [x_c = \sum_{i=1}^{\mathbb{M}_c} x_{(i,c)}/\mathbb{M}_c, y_c = \sum_{i=1}^{\mathbb{M}_c} y_{(i,c)}/\mathbb{M}_c]^T$. Accordingly, the energy consumption of v_j to flight towards cluster c in $d_{c,j}$ meters is calculated as

$$E_{(i,c)j}^f = E_0 d_{c,j}, \quad (14)$$

where E_0 is the required energy for flying per meter unit which is given as [47]

$$E_0 = P_0 \left(\frac{1}{V} + \frac{3V}{U_{tip}^2} \right) + P_{in} \left(\sqrt{V^{-4} + \frac{1}{4V_0^4}} - \frac{1}{2V_0^2} \right)^{\frac{1}{2}} + \frac{1}{2} d_0 \rho s A V^2, \quad (15)$$

where P_0 and P_{in} are the blade profile power and induced power in hovering status, respectively; V_0 denotes the mean rotor induced velocity in hover; ρ and A are known as the air density and rotor disc area, respectively. U_{tip} represents the tip speed of the rotor blade; d_0 stands for the fuselage drag ratio; and finally, s is the rotor solidity.

After arriving above cluster c , the UAV must adjust its flight altitude for which the UAV changes its altitude for \tilde{z}_j meter. It also can stay for a period of time with fixed power consumption above the cluster to process the tasks generated by TNs. By respectively considering e_{fa} and P_h as the required energy for adjusting one meter and the power consumption of the UAV for hovering in Watt, the energy consumption for flight altitude adjustment and hovering by v_j is calculated as

$$E_j^{\text{alt}} = \overbrace{e_{fa} \tilde{z}_j}^{\text{adjusting}} + \underbrace{P_h \tau}_{\text{hovering}}, \quad (16)$$

where τ shows the time that v_j spends to hover, which is known as the time-slot duration in this paper. Overall, the total energy consumption of v_j is given as

$$E_{c,j}^t = E_0 d_{c,j} + e_{fa} \tilde{z}_j + P_h \tau. \quad (17)$$

(2) Computing Energy Consumption

By considering P_j^{prc} as the power of processing one bit, the required energy for processing a task of size $L_{(i,c)}$ at v_j is calculated as

$$E_{(i,c)j}^{comp} = P_j^{prc} \frac{L_{(i,c)}}{\mu_j - \lambda_j L_j}. \quad (18)$$

(3) Energy Harvesting Model

LEO satellites, as the manager FNs, are able to manage the UAVs, by which they have access to the status of the UAVs. When the remaining energy of a UAV degrades a threshold, E_{th} , the corresponding LEO satellite starts transferring the energy to the UAV. The received power at v_j is given by $P_j^{rx} = |\mathbf{w}_k^H \mathbf{g}_{kj}|^2$, where $\mathbf{w}_k \in \mathbb{C}^{N_x \times N_y}$ is the energy beamforming vector [48] of s_k . We adopt a piece-wise linear EH model [49], in which the harvested power is linearly boosted with the received power up to a threshold, called the saturation point. Let η_j and P_{sat} show the linear energy conversion efficiency and the saturation power, respectively. Therefore, the harvested energy by v_j is modeled as

$$p_j^h = \begin{cases} \eta_j P_j^{rx} & 0 \leq \eta_j P_j^{rx} < P_{sat} \\ P_{sat} & \eta_j P_j^{rx} \geq P_{sat} \end{cases} \quad (19)$$

4.6 Throughput Model

Totally, there are T time slots in the system each with a size of τ in which the TNs offload their tasks to the corresponding UAV and then, the UAV decides how to process them. Figure 3 shows the block structure of the considered system model with respect to UAV v_j and its corresponding cluster, in which a time slot of size τ is divided into three phases as follows:

- *Initializing Phase:* At the beginning of each time slot, the cluster is formed, the UAV is associated with the cluster, and adjusts its 3D placement accordingly. It takes long τ_0 time units.
- *Pure Transmission Phase:* During this phase, the TNs transmit their tasks to the UAV. It is assumed that $n \leq \mathbb{M}_c$ TNs offload their tasks to the UAV. The time allocated to each TN is divided into two parts: one for transmitting the tasks from the TN to the UAV; and the other for processing the tasks. The total duration of this phase is shown by τ_{tx} .
- *Harvesting Phase:* Harvesting phase is started if the remaining energy of v_j , E_j^{rem} , is less than the predefined threshold, E_{th} . The total duration of this phase is

considered to be τ_{EH} , where is divided into two parts: in the first part, it takes long $\rho\tau_{EH}$ time units that the corresponding LEO satellite transfer the energy to the UAV, where ρ is a variable between 0 and 1; in the next $(1-\rho)\tau_{EH}$ time units, the rest of TNs offload their tasks to the UAV and the UAV processes the tasks.

Considering the above mentioned assumptions, throughput of $TN_{(i,c)}$ is modeled as

$$\mathcal{T}_{(i,c)j} = B \log_2 \left(1 + \frac{P_{(i,c)} g_0 \tilde{h}_{(i,c)j} d_{(i,c)j}^{-\alpha}}{I_{(i,c)}} \right) |t_{(i,c)}|, \quad (20)$$

where $|t_{(i,c)}|$ stands for the time allocated to the TN for transmission, which is given as

$$|t_{(i,c)}| = \begin{cases} \frac{\tau - \tau_{EH} - \tau_0}{2n} & \tau_0 < t_{(i,c)} \leq \tau_0 + \tau_{tx} \\ \frac{(1-\rho)\tau_{EH}}{2(\mathbb{M}_c - n)} & \tau_0 + \tau_{tx} < t_{(i,c)} \leq \tau \end{cases} \quad (21)$$

The throughput of v_j is defined in terms of the number of bits it processes that includes two parts: one is related to the number of bits processed before harvesting the energy, corresponding to the current energy of v_j , i.e., E_j^{curr} ; and the other is the number of bits processed after receiving the harvesting power. The total throughput of v_j is given as (22).

before harvesting part in (22) includes the number of bits processed at v_j . It implies that if the current energy of v_j is more than the required energy for processing all tasks generated by all TNs, then all bits are processed in this time portion; otherwise, $E_j^{curr} / \sum_{i=1}^n v_{(i,c)} E_{(i,c)j}$ portion of bits are processed and the rest are processed after harvesting the energy.

after harvesting part in (22) on the other hands obtains the number of unprocessed bits in the *before harvesting* plus the number of bits that can be processed based on the harvested power and the remaining energy of v_j .

5. Proposed Task Allocation Protocol

In this section, we propose a novel task allocation protocol, called Task allocation Protocol (TOP), for the H²TEC to efficiently adjust the 3D placement of the UAVs and assign the tasks to the available server nodes in the network such that the network performance is improved in terms of energy consumption and delay.

Although TOP focuses on the energy consumption and the delay in the network, what distinguishes TOP from the existing methods is the approach that TOP employs to improve the network throughput. TOP indeed takes advantage of EH in order to provide a supplementary energy budget for the UAVs by which more bits are processed by them. Moreover, the transmission rate of the TNs is adjusted in a way that these nodes can transmit more bits in the network. Overall, TOP comprises two phases, namely UAV's 3D placement adjustment phase, and task allocation phase, which are explained in the rest of this section.

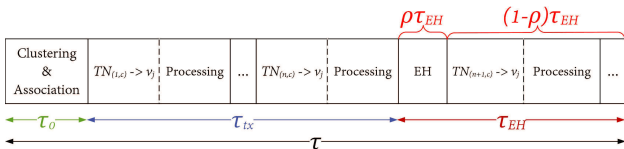


Fig. 3 Block structure of the considered system model.

$$\mathcal{T}_j = \underbrace{A_2 \sum_{i=1}^n v_{(i,c)} L_{(i,c)}}_{\text{before harvesting}} + \underbrace{(1 - A_2) \sum_{i=1}^n v_{(i,c)} L_{(i,c)} + \frac{(1 - \rho) \tau_{EH} \sum_{i=n+1}^{\mathbb{M}_c} L_{(i,c)}^2 P_j^h}{2A_3 \left(\sum_{i=n+1}^{\mathbb{M}_c} v_{(i,c)} E_{(i,c)} - E_j^{rem} \right)}}_{\text{after harvesting}}, \quad (22)$$

where $A_2 = \min \left\{ \frac{E_j^{curr}}{\sum_{i=1}^n v_{(i,c)} E_{(i,c)}}, 1 \right\}$, $A_3 = (\mu_j - \lambda_j L_j) \sum_{i=n+1}^{\mathbb{M}_c} v_{(i,c)} L_{(i,c)}$.

5.1 UAVs' 3D Placement Adjustment

At the beginning of each time slot, the TNs form the corresponding cluster and a UAV is assigned to each cluster. After the association of the UAV and the corresponding cluster, the UAV must adjust its 3D placement, i.e., the horizontal projection and the flight altitude, such that the TNs consume the minimum energy for transmitting their tasks to the UAV. According to the assumptions of the considered system model, the transmission power of all TNs in the network is fixed, while they experience a variable transmission rate in their transmission. Therefore, and according to (13), the transmission rate of the TNs has a direct effect on their energy consumption. Hence, finding the optimal transmission rate for each TN within a cluster results in the energy consumption optimization of the TNs.

However, the transmission rate of TNs within a cluster needs to be adjusted such that QoS requirements are provided in the network. One of the most important requirements is the outage probability which must be less than a threshold, β . Therefore, we have

$$R_{(i,c)} \leq B \log_2 \underbrace{\left(1 + \frac{\Gamma^{1/m}(m) \left(\beta + \frac{\Gamma(m, m\hbar^2)}{\Gamma(m)} \right)^{1/2m}}{m^{\left(\frac{m-1}{2m}\right)} \Gamma^{1/2m}(2m, m\hbar^2) A_4} \right)}_{R_{(i,c)}^{up,op}}. \quad (23)$$

where $A_4 = d_{(i,c)j}^\alpha \sum_{\substack{i'=1 \\ i' \neq i}}^{\mathbb{M}_c} d_{(i',c)j}^{-\alpha}$.

The other major requirement is the network reliability which needs to be more than a threshold, Υ_{th} . Hence, we have

$$R_{(i,c)} \leq \underbrace{\frac{-\omega_{(i,c)j} L_{(i,c)} (\mu_j - \lambda_j L_j)}{(\mu_j - \lambda_j L_j) \log_2 \Upsilon_{th} + \vartheta_j L_{(i,c)}}}_{R_{(i,c)}^{up,re}}. \quad (24)$$

One of the main contributions behind this work is to minimize the energy consumption of TNs in the network. To this end, the following problem is formulated in which the optimality of the energy consumption of the TNs depends

on the optimality of transmission rate of the TNs, as well as the flight altitude of the corresponding UAV. Since the clusters are independent of each other, the following problem is performed for each cluster, separately.

$$(P1): \underset{R_{(i,c)}, z_j}{\text{minimize}} \sum_{i=1}^{\mathbb{M}_c} v_{(i,c)} P_{(i,c)} \frac{L_{(i,c)}}{R_{(i,c)}} \quad (25)$$

s.t.

$$R_{(i,c)} \leq \min \left\{ R_{(i,c)}^{up,op}, R_{(i,c)}^{up,re} \right\}, \forall i \in c \quad (25a)$$

$$z_j^2 + \|\mathbf{u}_j - \mathbf{u}_{(i,c)}\|^2 \leq \mathcal{R}^2, \forall i \in c \quad (25b)$$

$$z_j^{min} \leq z_j; 0 < R_{(i,c)}, \forall i \in c \quad (25c)$$

The objective function focuses on minimizing the energy consumption of TNs within a cluster with respect to the transmission rate of the TNs and the flight altitude of the corresponding UAV. The proposed TOP aims at improving network reliability and avoid network outage probability. To this end, (25a) is defined to limit the transmission rate of each TN to the minimum value of two upper bounds: one that guarantees the reliability, and the other prevents the outage probability. Constraint (25b) implies that all TNs belong to cluster c must be under coverage of the corresponding UAV v_j . Finally, (25c) shows the boundaries of the objective variables, in which z_j^{min} is the minimum flight altitude that UAVs are allowed to fly over that.

5.1.1 Convergence, Optimality, and Complexity

The objective function is defined in terms of $R_{(i,c)}$. The Hessian of the objective function is given in (26) which is non-negative. Therefore, the objective function is convex.

$$f(P1) = \sum_{i=1}^{\mathbb{M}_c} v_{(i,c)} P_{(i,c)} \frac{L_{(i,c)}}{R_{(i,c)}} \rightarrow \quad (26)$$

$$\frac{d^2 f(P1)}{dR_{(i,c)}} = \sum_{i=1}^{\mathbb{M}_c} 2v_{(i,c)} P_{(i,c)} \frac{L_{(i,c)}}{R_{(i,c)}^3}$$

Constraint (25b) is convex as well. The bottleneck of P1 refers to (25a). According to (25a), there is a correlation between $R_{(i,c)}$ and z_j so that by increasing z_j , $R_{(i,c)}$ decreases

Algorithm 1 Optimal 3D Placement of the UAV v_j

```

1: Input:  $\mathcal{R}, z_j^{max}, z_j, \mathbb{M}_c, \mathbf{u}_{(i,c)}, \forall i \in c, \epsilon > 0;$ 
2:  $x_c = \sum_{i=1}^{\mathbb{M}_c} x_{(i,c)} / \mathbb{M}_c;$ 
3:  $y_c = \sum_{i=1}^{\mathbb{M}_c} y_{(i,c)} / \mathbb{M}_c;$ 
4:  $\mathbf{u}_c = [x_c \ y_c]^T;$ 
5:  $\mathbf{u}_j^* = \mathbf{u}_c;$ 
6:  $z_{min} = z_j;$ 
7:  $z_{max} = z_j^{max};$ 
8: Coverage  $(\mathbb{M}_c, z_j, \mathbf{u}_j^*, \mathbf{u}_{(1,c)}, \dots, \mathbf{u}_{(\mathbb{M}_c,c)}, \mathcal{R});$ 
9: if covered ==  $\mathbb{M}_c$  then
10:    $z_{min} = z^{min};$ 
11:    $z_{max} = z_j;$ 
12: end if
13: repeat
14:    $z_m = \lfloor (z_{min} + z_{max}) / 2 \rfloor;$ 
15:   Coverage  $(\mathbb{M}_c, z_m, \mathbf{u}_j^*, \mathbf{u}_{(1,c)}, \dots, \mathbf{u}_{(\mathbb{M}_c,c)}, \mathcal{R});$ 
16:   if covered <  $\mathbb{M}_c$  then
17:      $z_{min} = z_m;$ 
18:   else
19:      $z_{max} = z_m;$ 
20:   end if
21: until (covered -  $\mathbb{M}_c < 0$ )
22:  $z_j^* = z_m;$ 
23: for  $i = 1 : \mathbb{M}_c$  do
24:   Calculate  $R_{(i,c)}^{up,op}$  by using (23);
25:    $R_{(i,c)}^* = \min \{ R_{(i,c)}^{up,op}, R_{(i,c)}^{up,re} \};$ 
26: end for
27: Return  $\mathbf{u}_j^*, z_j^*, R_{(1,c)}^*, \dots, R_{(\mathbb{M}_c,c)}^*;$ 

```

Function Coverage $(\mathbb{M}_c, z, \mathbf{u}_j^*, \mathbf{u}_{(1,c)}, \dots, \mathbf{u}_{(\mathbb{M}_c,c)}, \mathcal{R})$

```

1: Initialize covered = 0;
2: for  $i = 1 : \mathbb{M}_c$  do
3:   if  $z^2 + \|\mathbf{u}_j^* - \mathbf{u}_{(i,c)}\|^2 \leq \mathcal{R}^2$  then
4:     covered = covered + 1;
5:   end if
6: end for
7: Return covered;

```

and vice versa. Hence, optimizing $R_{(i,c)}$ directly depends on optimizing z_j . The objective function is minimized if $R_{(i,c)}$ reaches its maximum value, i.e., $\min\{R_{(i,c)}^{up,op}, R_{(i,c)}^{up,re}\}$ for which the corresponding UAV v_j must decrease its distance from the corresponding TNs. The optimal horizontal projection of v_j to cover all TNs within a cluster is the cluster centroid. Therefore, $\mathbf{u}_j^* = \mathbf{u}_c$. By decreasing the flight altitude by v_j , its coverage range also decreases. Therefore, the minimum altitude of v_j is the altitude that the farthest TN is under cover of v_j . Subsequently, the objective function is maximized when the transmission rate of the farthest TN is maximized for which v_j must adjust its flight altitude until the farthest TN is under its coverage.

Algorithm 1 shows the procedure of obtaining the optimal transmission rate for TNs and the optimal flight altitude for the corresponding UAV by using the bisection algorithm. As can be seen in lines 2–5, the algorithm calculates the horizontal coordinate of the cluster and assigns it as the opti-

mal horizontal projection of v_j . Then, the algorithm assigns the values of z_{min} and z_{max} as the boundaries of the UAV's flight altitude. To this end, the algorithm runs the Coverage function to check if the TNs are within the coverage area of the UAV at the current altitude, z_j . If so, it sets the upper boundary as the current altitude, i.e., $z_{max} = z_j$ and the lower boundary as a very small positive value shown by ϵ , i.e., $z_{min} = \epsilon$. This condition implies that the UAV decreases its altitude until the TNs are under its coverage and (25a) is met. On the other hand, the UAV must increase its altitude such that all TNs are under its coverage for which it sets the boundaries as $z_{max} = z_j^{max}$ and $z_{min} = z_j$, where z_j^{max} is the maximum legal flight altitude introduced by the government up to which a UAV can fly.

By considering $\epsilon = \mathbb{M}_c - \text{covered}$, the complexity of Algorithm 1 will be $O(\mathbb{M}_c(\log \epsilon)/2)$.

5.2 Throughput Maximization

When a UAV receives a task from the TNs, it first checks the delay constraint of the task to decide if the UAV can process the task locally. Therefore, there would be two different conditions:

- *Offloading*: If the task's processing delay exceeds a threshold, D_{th} , the UAV offloads the task to either the corresponding LEO satellite or the corresponding terrestrial BS. In the case that the UAV is flying over the areas without any BSs, the LEO satellite after receiving the task decides to process it locally or offload the to the GEO satellite for further process. On the other hand, If the BS receives the task, it also decides to process the task locally, offload it to a neighbor UAV, or forward it to the cloud center. Each BS can cover a specific area based on its coverage range. In H²TEC, the UAVs cannot directly communicate with each other. Hence, the communication is done by the corresponding BS. All of the aforementioned decisions depend on the delay constraint of the task and the resource availability of the nodes.
- *Local Processing*: If the task's processing delay is less than D_{th} , the UAV processes the task locally. However, the limited energy budget of the UAV imposes some limitations on the local processing of the tasks. To deal with this issue, the corresponding LEO satellite that manages the UAV starts transferring the energy to the UAV whenever the remaining energy of the UAV is less than the predefined threshold E_{th} , i.e., $E_j^{rem} < E_{th}$.

In the case of local processing, the optimal amount of harvested energy and the time of EH play important roles in maximizing the network throughput. By considering throughput of $TN_{(i,c)}$ and the corresponding UAV v_j respectively defined in (20) and (22), the following problem formulation is proposed to maximize total network throughput with respect to the harvested power P_j^h , the energy beamforming vector, \mathbf{w}_k , and the appropriate portion of time assigned for EH, i.e., ρ .

$$\begin{aligned}
f(P2) &= B \sum_{i=n+1}^{\mathbb{M}_c} \log_2 \left(1 + \frac{P_{(i,c)} g_0 \tilde{h}_{(i,c)j} d_{(i,c)j}^{-\alpha}}{I_{(i,c)}} \right) \frac{(1-\rho) \tau_{EH}}{2(\mathbb{M}_c - n)} + \\
&\quad \frac{(1-\rho) \tau_{EH} \sum_{i=n+1}^{\mathbb{M}_c} L_{(i,c)}^2 P_j^h}{2 \left((\mu_j - \lambda_j L_j) \sum_{i=n+1}^{\mathbb{M}_c} \nu_{(i,c)} L_{(i,c)} \right) \left(\sum_{i=n+1}^{\mathbb{M}_c} \nu_{(i,c)} E_{(i,c)} - E_j^{rem} \right)} \quad (28) \\
&\quad \underbrace{\hspace{15em}}_{f_2(P2)}
\end{aligned}$$

$$(P2): \underset{\rho, \mathbf{w}_k, P_j^h}{\text{maximize}} \sum_{i=1}^{\mathbb{M}_c} \mathcal{T}_{(i,c)j} + \bar{\mathcal{T}}_j \quad (27)$$

s.t.

$$\rho P_j^h \geq \left(\frac{P_j^{Pr c} \sum_{i=n+1}^{\mathbb{M}_c} \nu_{(i,c)} L_{(i,c)}}{(\mathbb{M}_c - n)(\mu_j - \lambda_j L_j)} \right) \times \frac{2}{\tau_{EH}} \quad (27a)$$

$$P_j^h \leq \min \{ \eta_j |\mathbf{w}_k^H \mathbf{g}_{kj}|^2, P_{sat} \} \quad (27b)$$

$$\text{Tr}(\mathbf{w}_k \mathbf{G}_{kj} \mathbf{w}_k^H) \leq P_k \quad (27c)$$

$$0 \leq \rho \leq 1 \quad (27d)$$

The objective function of P2 aims to maximize the throughput. Constraint (27a) implies that the harvested energy needs to be more than the required energy for processing the tasks locally. Constraint (27b) determines the upper boundary of the harvesting power. According to (27c), the transformed power by the LEO satellite s_k cannot exceed the allowable transmission power of s_k , i.e., P_k . It is noticeable that $\mathbf{G}_{kj} = \mathbf{g}_{kj} \mathbf{g}_{kj}^H$. Finally, (27d) shows that the value of ρ changes between 0 and 1.

5.2.1 Convergence, Optimality, and Complexity

The main objective of the proposed model P2 is to jointly optimize the energy transfer duration and the harvested energy in each time slot such that the total network throughput is maximized. To this end, we manipulate the objective function provided in (27) to rewrite it in form of the functions which include the objective variables. The new form of the objective function is shown in (28), where the objective function comprises two parts, shown as $f_1(P2)$ and $f_2(P2)$. $f_1(P2)$ function is a linear function of ρ , that is convex; $f_2(P2)$ on the other hand is a function of combination of P_j^h and ρ . This implies that $f_1(P2)$ is non-convex. To solve this problem, it is assumed that ρ is fixed. We solve the problem in terms of P_j^h to find optimal harvested power, i.e., $P_j^{h,*}$. Then, the optimal value of ρ , i.e., ρ^* , is found based on $P_j^{h,*}$.

(1) Optimal Harvested Power

According to constraints provided in P2, P_j^h is a function of

Algorithm 3 Throughput Maximization Algorithm

- 1: **Initialize:** ρ ;
 - 2: Relax (29c) and solve P2.2 by CVX;
 - 3: Find \mathbf{w}_k^* by using the Gaussian randomization method;
 - 4: Find $P_j^{h,*}$ by solving P2.3 with respect to the obtained \mathbf{w}_k^* ;
 - 5: Find ρ^* by solving P2.3 with respect to the obtained $P_j^{h,*}$;
 - 6: Return $P_j^{h,*}, \rho^*$;
-

\mathbf{w}_k . To find the optimal value of P_j^h , we need to find the optimal value of \mathbf{w}_k , i.e., \mathbf{w}_k^* . Although the objective function in (28) is convex due to the linear relationship between the function and P_j^h , constraints (27b) and (27c) are quadratically constrained quadratic program (QCQP), that causes the problem to be a nonconvex problem. To turn the nonconvex problem into a convex problem, a new variable is introduced as $\mathbf{W}_k = \mathbf{w}_k \mathbf{w}_k^H$, where \mathbf{W}_k is a rank-one symmetric positive semidefinite (PSD) matrix [50]. By substituting \mathbf{W}_k in P2, we have

$$(P2.1): \underset{\rho, \mathbf{W}_k, P_j^h}{\text{maximize}} f_2(P2) \quad (29)$$

s.t. (27a),

$$P_j^h \leq \min \{ \eta_j \text{Tr}(\mathbf{W}_k \mathbf{G}_{kj}), P_{sat} \} \quad (29a)$$

$$\text{Tr}(\mathbf{W}_k \mathbf{G}_{kj}) \leq P_k \quad (29b)$$

$$\text{Rank}(\mathbf{W}_k) = 1 \quad (29c)$$

$$\mathbf{W}_k \geq 0 \quad (29d)$$

The objective function is maximized if P_j^h reaches its maximum value. According to (29a), P_j^h is maximized when $\eta_j \text{Tr}(\mathbf{W}_k \mathbf{G}_{kj})$ is maximized. Therefore, we first solve the following problem to find the optimal value of \mathbf{W}_k .

$$(P2.2): \underset{\mathbf{W}_k}{\text{maximize}} \text{Tr}(\mathbf{W}_k \mathbf{G}_{kj}) \quad (30)$$

s.t. (29b), (29c), (29d)

To find the optimal value of \mathbf{w}_k , i.e., \mathbf{w}_k^* , the powerful efficient approximation method, called semidefinite relaxation (SDR) [50], is used by which the rank-one constraint on \mathbf{W}_k , i.e., (29c) is relaxed. The relaxed problem is a convex

semidefinite programming (SDP) problem that needs to be solved for which the convex optimization toolbox, namely CVX, can be used [50]. Accordingly, the optimal solution \mathbf{W}_k^* is found that might be of a rank greater than one. Therefore, in the next step, the Gaussian randomization method is employed to extract a feasible and optimal solution \mathbf{w}_k^* of rank one. Thereafter, the following problem is solved to find the optimal value of P_j^h , i.e., $P_j^{h,*}$.

$$(P2.3): \underset{P_j^h}{\text{maximize}} f_2(P2) \quad (31)$$

s.t. (27a), (27b)

(2) Optimal Energy Transfer Duration

After finding the optimal harvested power, we need to find the optimal portion of energy transfer duration, i.e., ρ^* . This could be achieved by solving the following problem:

$$(P2.4): \underset{\rho}{\text{maximize}} \sum_{i=1}^{M_c} \mathcal{T}_{(i,c)j} + \mathcal{T}_j \quad (32)$$

s.t. (27a), (27d)

(3) Throughput Maximization Algorithm

Algorithm 3 summarized the procedure of finding $P_j^{h,*}$ and ρ^* for which (27a) is relaxed and P2.2 is solved by CVX. Then, \mathbf{w}_k^* is extracted from the obtained optimal \mathbf{W}_k^* by using the Gaussian randomization method. Accordingly, solving P2.3 gives the optimal $P_j^{h,*}$. Finally, ρ^* is given by solving P2.4 with respect to the obtained $P_j^{h,*}$.

The complexity of the throughput maximization algorithm follows the complexity of solving the SDP problem in CVX that is polynomial in terms of the number of LEOs' antennas, i.e., N_x and N_y .

6. Numerical Results

We consider a system in which $M = 10000$ TNs are uniformly distributed in a region with a radius of $r = 2000$ m. Considering a given coverage radius of $\mathcal{R} = 200$ m every single UAV, optimal number of clusters (or equivalently, number of UAVs) to cover all TNs is given as

$$N^* = \left(\frac{r}{\mathcal{R}}\right)^2 \quad (33)$$

Proof. The density of nodes in a region with the radius of r is equal to $M/(\pi r^2)$. Each UAV with a radius of \mathcal{R} can cover $M/(\pi r^2) \times \pi \mathcal{R}^2$. For M TNs, $M/(M/(\pi r^2) \times \pi \mathcal{R}^2)$ UAVs are required to provide the services. By simplification, totally $N^* = (r/\mathcal{R})^2$ UAVs are needed. \square

Each TN $_{(i,c)}$ generates $\nu_{(i,c)} = U[100, 200]$ tasks in each time slot. The size of tasks follows a uniform distributed value between 60 and 80 KB. All TNs have the same maximum transmission power, which is equal to 23 dBm [45]. The rotary UAVs are considered, where $E_0 = 55$ J/m and

Table 1 System setup for numerical simulations.

Parameter	B	α	β	Υ_{th}	P_k	z^{max}	z^{min}
Value	10 MHz	3	0.01	0.99	80 W	120 m	30 m

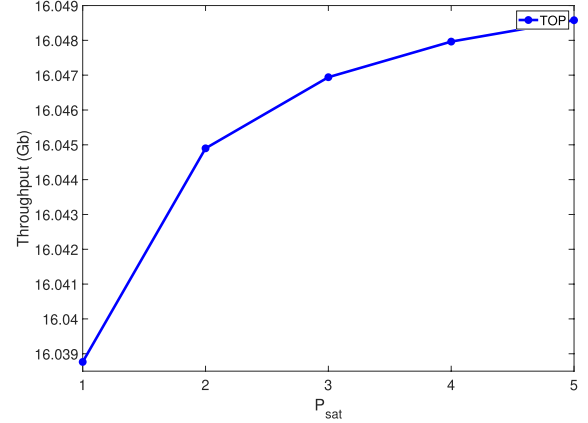


Fig. 4 Throughput vs. P_{sat} .

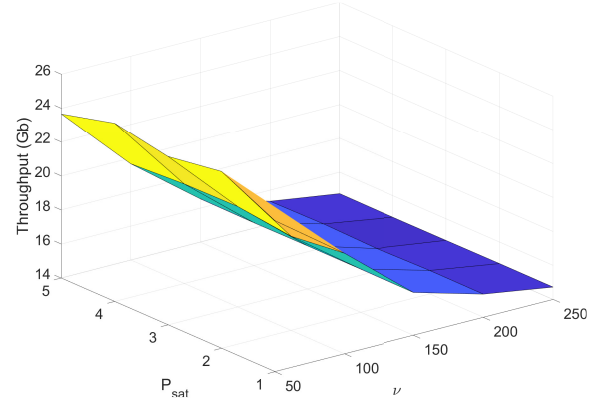


Fig. 5 Throughput with respect to the saturation power, P_{sat} , and the traffic rate ν .

$P_h = 170$ W [34]. The following setup is used for other network parameters: $\mu_j = 100$ Mbps, $\vartheta_j = U[0.001, 0.3]$, $\eta_j = 0.2 \forall j$; $\omega_{(i,c)j} = U[0.001, 0.3] \forall i, c, j$. We assume that \mathbf{w}_k and \mathbf{g}_{kj} are symmetric, i.e., $N_x = N_y$. Besides, the channel gain between the satellites and the UAVs follows the SR distribution with parameters (0.126, 10, 0.835) [27]. The CVX toolbox of MATLAB has been used to develop the simulation models. The rest of simulation parameters are given in Table 1.

In the first step, we show the impact of the saturation power on the network throughput. To this end, we perform the simulations for different values of P_{sat} . Figure 4 shows the corresponding results where, by increasing the saturation power of the UAVs, these nodes can harvest more energy. Subsequently, the UAVs have more energy to process more bits, and hence, the network throughput increases.

The other parameter that can affect the network throughput is the traffic rate of the TNs. The obtained results in Fig. 5

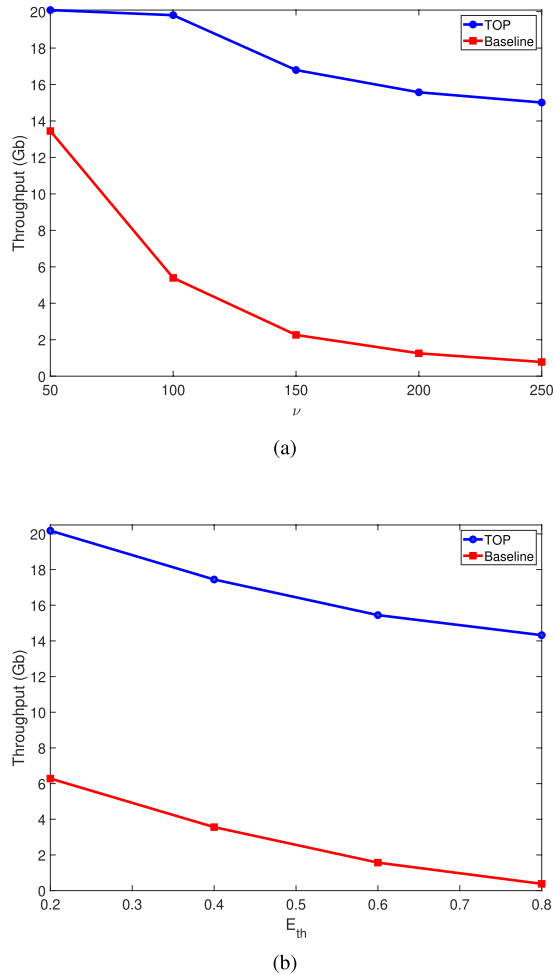


Fig. 6 Comparison of the proposed TOP and the benchmark method with respect to: (a) the traffic rate of TNs, ν ; and (b) the threshold energy of UAVs, E_{th} .

imply that increasing the number of generated tasks by the TNs leads to the reduction of the network throughput. The reason arose from that according to the assumption of the considered system model, TNs offload all their tasks to the corresponding UAV in order during a time slot. Accordingly, the first TN offloads the tasks as the first node; thereafter, the second TN sends all its tasks; and this procedure continues until the UAV has enough energy to process the incoming tasks from the TNs. Although the proposed TOP makes it possible to harvest the energy from the satellites to process more tasks, the limited time duration does not allow the UAVs to process all available tasks in a time slot. Therefore, the network throughput decreases.

Also, we compare the proposed TOP with a baseline scheme in which the UAVs do not harvest the energy from the satellites. Figure 6 shows the corresponding results. We first consider the scenario with different traffic rates of TNs. As seen in Fig. 6(a), by increasing the traffic rates of the TNs, the network throughput decreases. However, due to the capability of the UAVs in harvesting the energy from the satellites, the TOP achieves high network throughput

even in high data traffic. This is while the throughput is about zero for the baseline mechanism. On the other hand, we have set the threshold energy of the UAVs, E_{th} , to a portion of their initial energy. Figure 6(b) indicates that E_{th} changes from 20% to 80% of the initial energy of UAVs. Accordingly, the network throughput is decreased for both methods. However, the energy harvesting provided in the TOP causes a slight deduction of the network throughput compared to the baseline scheme.

7. Conclusion

In this paper, we proposed a novel architecture, named H²TEC, for the IoT networks, in which the UAVs can provide the services for the TNs in cooperation with the satellites, especially where the access to the stationary BSs is hard or impossible for the TNs. Accordingly, the novel Task allocation Protocol (TOP) was proposed, where the optimal transmission rate of the TNs is set so that the outage probability of the network is guaranteed, the network reliability is ensured, and the TNs consume the minimum energy for offloading the tasks to the corresponding UAV. Moreover, TOP enables the energy harvesting for the UAVs by which the LEO satellites transfer the energy to the UAVs when the remaining energy of the UAVs is below a predefined threshold. Therefore, the UAVs can process more bits by assigning the optimal harvested power, as well as the optimal portion of the harvesting time. Numerical results reveal that TOP could improve the network throughput in various scenarios with respect to different parameters.

References

- [1] C. Mouradian, D. Naboulsi, S. Yangui, R.H. Glitho, M.J. Morrow, and P.A. Polakos, "A comprehensive survey on fog computing: State-of-the-art and research challenges," *IEEE Commun. Surveys Tuts.*, vol.20, no.1, pp.416–464, 2018.
- [2] A. Yousefpour, G. Ishigaki, R. Gour, and J.P. Jue, "On reducing IoT service delay via fog offloading," *IEEE Internet Things J.*, vol.5, no.2, pp.998–1010, 2018.
- [3] F.S. Abkenar and A. Jamalipour, "EBA: Energy balancing algorithm for fog-IoT networks," *IEEE Internet Things J.*, vol.6, no.4, pp.6843–6849, 2019.
- [4] M. Mukherjee, Y. Liu, J. Lloret, L. Guo, R. Matam, and M. Aazam, "Transmission and latency-aware load balancing for fog radio access networks," 2018 *IEEE Global Communications Conference (GLOBECOM)*, pp.1–6, 2018.
- [5] F. Shirin Abkenar and A. Jamalipour, "Energy optimization in association-free fog-IoT networks," *IEEE Trans. Green Commun. Netw.*, vol.4, no.2, pp.404–412, 2020.
- [6] F.S. Abkenar, K.S. Khan, and A. Jamalipour, "Smart-cluster-based distributed caching for fog-iot networks," *IEEE Internet Things J.*, vol.8, no.5, pp.3875–3884, 2021.
- [7] D.T. Hoang, D. Niyato, D.N. Nguyen, E. Dutkiewicz, P. Wang, and Z. Han, "A dynamic edge caching framework for mobile 5G networks," *IEEE Wireless Commun.*, vol.25, no.5, pp.95–103, 2018.
- [8] N. Raveendran, H. Zhang, L. Song, L.C. Wang, C.S. Hong, and Z. Han, "Pricing and resource allocation optimization for IoT fog computing and NFV: An EPEC and matching based perspective," *IEEE Trans. Mobile Comput.*, p.1, 2020.
- [9] F.S. Abkenar, M.Z. Alam, and A. Jamalipour, "Transaction through-

- put maximization under delay and energy constraints in fog-IoT networks," *GLOBECOM 2020 - 2020 IEEE Global Communications Conference*, pp.1–6, 2020.
- [10] P. Ramezani, Y. Zeng, and A. Jamalipour, "Optimal resource allocation for multiuser internet of things network with single wireless-powered relay," *IEEE Internet Things J.*, vol.6, no.2, pp.3132–3142, 2019.
- [11] P. Ramezani and A. Jamalipour, "Optimal resource allocation in backscatter assisted WPCN with practical energy harvesting model," *IEEE Trans. Veh. Technol.*, vol.68, no.12, pp.12406–12410, 2019.
- [12] X. Hou, Y. Li, M. Chen, D. Wu, D. Jin, and S. Chen, "Vehicular fog computing: A viewpoint of vehicles as the infrastructures," *IEEE Trans. Veh. Technol.*, vol.65, no.6, pp.3860–3873, 2016.
- [13] M. Mozaffari, W. Saad, M. Bennis, Y. Nam, and M. Debbah, "A tutorial on UAVs for wireless networks: Applications, challenges, and open problems," *IEEE Commun. Surveys Tuts.*, vol.21, no.3, pp.2334–2360, 2019.
- [14] J. Guo and Y. Du, "Fog service in space information network: Architecture, use case, security and challenges," *IEEE Access*, vol.8, pp.11104–11115, 2020.
- [15] J. Liu, Y. Shi, Z.M. Fadlullah, and N. Kato, "Space-air-ground integrated network: A survey," *IEEE Commun. Surveys Tuts.*, vol.20, no.4, pp.2714–2741, 2018.
- [16] M.A. Ali and A. Jamalipour, "Uav placement and power allocation in uplink and downlink operations of cellular network," *IEEE Trans. Commun.*, vol.68, no.7, pp.4383–4393, 2020.
- [17] X. Wei, C. Tang, J. Fan, and S. Subramaniam, "Joint optimization of energy consumption and delay in cloud-to-thing continuum," *IEEE Internet Things J.*, vol.6, no.2, pp.2325–2337, 2019.
- [18] G. Wu, Y. Miao, Y. Zhang, and A. Barnawi, "Energy efficient for UAV-enabled mobile edge computing networks: Intelligent task prediction and offloading," *Comput. Commun.*, vol.150, pp.556–562, 2020.
- [19] J. Xiong, H. Guo, and J. Liu, "Task offloading in UAV-aided edge computing: Bit allocation and trajectory optimization," *IEEE Commun. Lett.*, vol.23, no.3, pp.538–541, 2019.
- [20] X. Wang, W. Feng, Y. Chen, and N. Ge, "Sum rate maximization for mobile UAV-aided Internet of things communications system," 2018 IEEE 88th Vehicular Technology Conference (VTC-Fall), pp.1–5, 2018.
- [21] M. Alsenwi, Y.K. Tun, S. Raj Pandey, N.N. Ei, and C. Seon Hong, "UAV-assisted multi-access edge computing system: An energy-efficient resource management framework," 2020 International Conference on Information Networking (ICOIN), pp.214–219, 2020.
- [22] H. Xu, C. Pan, K. Wang, M. Chen, and A. Nallanathan, "Resource allocation for UAV-assisted IoT networks with energy harvesting and computation offloading," 2019 11th International Conference on Wireless Communications and Signal Processing (WCSP), pp.1–7, 2019.
- [23] N.T. Ti and L. Bao Le, "Joint resource allocation, computation offloading, and path planning for UAV based hierarchical fog-cloud mobile systems," 2018 IEEE Seventh International Conference on Communications and Electronics (ICCE), pp.373–378, 2018.
- [24] A. Pandey, D. Kushwaha, and S. Kumar, "Energy efficient UAV placement for multiple users in IoT networks," 2019 IEEE Global Communications Conference (GLOBECOM), pp.1–6, 2019.
- [25] M. Mozaffari, W. Saad, M. Bennis, and M. Debbah, "Optimal transport theory for cell association in UAV-enabled cellular networks," *IEEE Commun. Lett.*, vol.21, no.9, pp.2053–2056, 2017.
- [26] M. Mozaffari, W. Saad, M. Bennis, and M. Debbah, "Mobile unmanned aerial vehicles (UAVs) for energy-efficient internet of things communications," *IEEE Trans. Wireless Commun.*, vol.16, no.11, pp.7574–7589, 2017.
- [27] M. Hua, Y. Wang, M. Lin, C. Li, Y. Huang, and L. Yang, "Joint CoMP transmission for UAV-aided cognitive satellite terrestrial networks," *IEEE Access*, vol.7, pp.14959–14968, 2019.
- [28] N. Cheng, F. Lyu, W. Quan, C. Zhou, H. He, W. Shi, and X. Shen, "Space/aerial-assisted computing offloading for IoT applications: A learning-based approach," *IEEE J. Sel Areas Commun.*, vol.37, no.5, pp.1117–1129, 2019.
- [29] S. Mao, S. He, and J. Wu, "Joint UAV position optimization and resource scheduling in space-air-ground integrated networks with mixed cloud-edge computing," *IEEE Syst. J.*, vol.15, no.3, pp.3992–4002, 2021.
- [30] S. Gu, Y. Wang, N. Wang, and W. Wu, "Intelligent optimization of availability and communication cost in satellite-UAV mobile edge caching system with fault-tolerant codes," *IEEE Trans. Cogn. Commun. Netw.*, vol.6, no.4, pp.1230–1241, 2020.
- [31] C. Joo and J. Choi, "Low-delay broadband satellite communications with high-altitude unmanned aerial vehicles," *J. Commun. Netw.*, vol.20, no.1, pp.102–108, 2018.
- [32] V. Nguyen, T.T. Khanh, P. Van Nam, N.T. Thu, C. Seon Hong, and E.-N. Huh, "Towards flying mobile edge computing," 2020 International Conference on Information Networking (ICOIN), pp.723–725, 2020.
- [33] Z. Wang, R. Liu, Q. Liu, J.S. Thompson, and M. Kadoch, "Energy-efficient data collection and device positioning in UAV-assisted IoT," *IEEE Internet Things J.*, vol.7, no.2, pp.1122–1139, 2020.
- [34] Y. Zeng, J. Xu, and R. Zhang, "Energy minimization for wireless communication with rotary-wing UAV," *IEEE Trans. Wireless Commun.*, vol.18, no.4, pp.2329–2345, 2019.
- [35] D.J. Bem, T.W. Wiecekowski, and R.J. Zielinski, "Broadband satellite systems," *IEEE Commun. Surveys Tuts.*, vol.3, no.1, pp.2–15, 2000.
- [36] K. Dredge, M. v. Arx, and I. Timmins, "LEO constellations and tracking challenges," *Satellite Evolution Magazine*, pp.36–38, Sept.-Oct. 2017. [Online]. Available: <https://www.satelliteevolutiongroup.com/magazines/SEA-Sept-Oct-2017/html5forpc.html?page=0>
- [37] S.T. Goh and S.A. Zekavat, "Space-based solar power via LEO satellite networks: Synchronization efficiency analysis," 2013 IEEE Aerospace Conference, pp.1–9, 2013.
- [38] J. Yu, X. Liu, Y. Gao, and X. Shen, "3D channel tracking for UAV-satellite communications in space-air-ground integrated networks," *IEEE J. Sel. Areas Commun.*, vol.38, no.12, pp.2810–2823, 2020.
- [39] R. Yamasaki and T. Tanaka, "Properties of mean shift," *IEEE Trans. Pattern Anal. Mach. Intell.*, vol.42, no.9, pp.2273–2286, 2020.
- [40] Y.J. Chun, S.L. Cotton, H.S. Dhillon, F.J. Lopez-Martinez, J.F. Paris, and S.K. Yoo, "A comprehensive analysis of 5G heterogeneous cellular systems operating over κ - μ shadowed fading channels," *IEEE Trans. Wireless Commun.*, vol.16, no.11, pp.6995–7010, 2017.
- [41] P.K. Sharma, D. Gupta, and D.I. Kim, "Cooperative AF-based 3D mobile UAV relaying for hybrid satellite-terrestrial networks," 2020 IEEE 91st Vehicular Technology Conference (VTC2020-Spring), pp.1–5, 2020.
- [42] C. Wang, X. Yang, Q. Du, and J. Wang, "Outage performance of satellite-UAV network framework based on NOMA," 2021 IEEE 5th International Conference on Cryptography, Security and Privacy (CSP), pp.171–175, 2021.
- [43] S. Iranmanesh, F.S. Abkenar, R. Raad, and A. Jamalipour, "Improving throughput of 5G cellular networks via 3D placement optimization of logistics drones," *IEEE Trans. Veh. Technol.*, vol.70, no.2, pp.1448–1460, 2021.
- [44] M. Horani and M.O. Hasna, "Latency analysis of UAV based communication networks," 2018 International Conference on Information and Communication Technology Convergence (ICTC), pp.385–390, 2018.
- [45] F.S. Abkenar and A. Jamalipour, "A reliable data loss aware algorithm for fog-IoT networks," *IEEE Trans. Veh. Technol.*, vol.69, no.5, pp.5718–5722, 2020.
- [46] X. Hou, Z. Ren, W. Cheng, C. Chen, and H. Zhang, "Fog based computation offloading for swarm of drones," ICC 2019 - 2019 IEEE International Conference on Communications (ICC), pp.1–7, 2019.
- [47] Y. Zeng, J. Xu, and R. Zhang, "Energy minimization for wireless communication with rotary-wing UAV," *IEEE Trans. Wireless Commun.*, vol.18, no.4, pp.2329–2345, 2019.
- [48] E. Björnson, M. Bengtsson, and B. Ottersten, "Optimal multiuser

transmit beamforming: A difficult problem with a simple solution structure [lecture notes],” *IEEE Signal Process. Mag.*, vol.31, no.4, pp.142–148, 2014.

- [49] P. Ramezani and A. Jamalipour, “Two-way dual-hop WPCN with a practical energy harvesting model,” *IEEE Trans. Veh. Technol.*, vol.69, no.7, pp.8013–8017, 2020.
- [50] Z.-Q. Luo, W.-K. Ma, A.M.-C. So, Y. Ye, and S. Zhang, “Semidefinite relaxation of quadratic optimization problems,” *IEEE Signal Process. Mag.*, vol.27, no.3, pp.20–34, 2010.



Abbas Jamalipour received the Ph.D. degree in Electrical Engineering from Nagoya University, Nagoya, Japan. He is a Professor of Ubiquitous Mobile Networking with the University of Sydney, Sydney, Australia. He has authored nine technical books, eleven book chapters, over 550 technical papers, and five patents, all in the area of wireless communications. Prof. Jamalipour is a recipient of the number of prestigious awards, such as the 2019 IEEE ComSoc Distinguished Technical Achievement Award in

Green Communications, the 2016 IEEE ComSoc Distinguished Technical Achievement Award in Communications Switching and Routing, the 2010 IEEE ComSoc Harold Sobol Award, the 2006 IEEE ComSoc Best Tutorial Paper Award, as well as 15 Best Paper Awards. He is the President of the IEEE Vehicular Technology Society (2020–2021). He held the positions of the Executive Vice-President and the Editor-in-Chief of VTS Mobile World and has been an elected member of the Board of Governors of the IEEE Vehicular Technology Society since 2014. He was the Editor-in-Chief IEEE WIRELESS COMMUNICATIONS, the Vice President-Conferences, and a member of Board of Governors of the IEEE Communications Society. He sits on the Editorial Board of the IEEE ACCESS and is an Editor of the IEEE TRANSACTIONS ON VEHICULAR TECHNOLOGY, and several other journals. He has been the General Chair or Technical Program Chair for a number of conferences, including IEEE ICC, GLOBECOM, WCNC, and PIMRC. He is a Fellow of the Institute of Electrical, Information, and Communication Engineers (IEICE), the Institute of Electrical and Electronics Engineering (IEEE), and the Institution of Engineers Australia; an ACM Professional Member, and an IEEE Distinguished Speaker.



Forough Shirin Abkenar received her B.Sc. and M.Sc. degrees in Information Technology in Iran. She is currently a Ph.D. candidate with the Wireless Networking Group (WiNG) at The University of Sydney, working under the supervision of Prof. Abbas Jamalipour. Forough’s research topic is to provide different quality of service (QoS) requirements such as energy efficiency, delay, and throughput in fog-enabled Internet of Things (IoT) networks. Her research interests include Fog computing, Internet of Things (IoT),

Internet of Vehicles (IoV), Unmanned aerial vehicles (UAVs), Machine learning (ML), and Elastic optical networks (EONs).